



A distributed model for continuous-wave erbium-doped fiber laser

Josue del Valle-Hernandez ^a, Yuri O. Barmenkov ^{a,*}, Stanislav A. Kolpakov ^b, Jose L. Cruz ^c, Miguel V. Andres ^c

^a Centro de Investigaciones en Óptica, Loma del Bosque 115, Col. Lomas del Campestre, León, 37150, Gto., Mexico

^b Departamento de Óptica, Universidad de Valencia, Dr. Moliner 50, 46100, Burjassot (Valencia), Spain

^c Departamento de Física Aplicada, ICMUV, Universidad de Valencia, Dr. Moliner 50, 46100, Burjassot (Valencia), Spain

ARTICLE INFO

Article history:

Received 21 April 2011

Received in revised form 5 June 2011

Accepted 24 July 2011

Available online 7 August 2011

Keywords:

Erbium-doped fiber

Fiber laser

Excited state absorption

Radial distribution

Distributed model

ABSTRACT

A distributed model of a continuous-wave erbium-doped fiber laser is discussed. The model is based on two contra-propagated traveling laser waves, and includes inhomogeneous pumping, excited state absorption at the pump and the laser wavelengths, amplified spontaneous emission and radial distribution of populations of erbium levels. It is shown that excited state absorption is a main limiting factor to the laser's efficiency. Moreover, consideration of radial distributions of erbium levels' populations in the model reduces laser efficiency and decreases optimal reflection of the laser output coupler. The modeling results are in excellent agreement with the experimental study on the EDFL efficiency.

© 2011 Elsevier B.V. All rights reserved.

1. Introduction

Erbium-doped fiber lasers (EDFLs) are popular light sources usually designed in all-fiber geometry, emitting in a broad spectral range covering the S, C, and L communication bands [1,2]. A variety of EDFL regimes have been demonstrated including multi-wavelength operation [3,4], stable Q-switching and mode-locking [5,6], narrow-line [7] and single-frequency [8,9] oscillation, wide-range wavelength tuning ability [1,10], etc. A special attention has been addressed to EDFLs in a linear configuration (Fabry–Perot cavity) that allows one to apply high-selective mirrors in a form of fiber Bragg gratings (FBGs) as cavity couplers. A number of papers were focused on modeling of such type of the fiber lasers (FLs). The most realistic models describing FLs are based on a distributed model [11,12], in which an amplifying medium is long. Usually the input laser coupler is of high reflectivity and the output one is of relatively low reflectivity [13]. The authors of these works analyzed FLs by analytical functions after corresponding simplification of the rate and laser equations.

It is known that EDFLs are not free from some disadvantages as, for example, their relatively low efficiency comparing to ytterbium-doped fiber lasers. The reason for this is the presence of excited state absorption (ESA) observed in Er-doped fibers (EDFs) at the pump and the laser wavelengths [14,15]. In such conditions EDFL cannot be described quantitatively by a simplified analytical model because ESA-induced loss depends on a distance along the active fiber (z -coordinate)

as a complex function of both the pump and laser generation powers that, in turn, also depend on z .

Our goal in this work is to introduce a distributed model of a linear-cavity EDFL with in-core pumping, in which ESA of erbium ions at the pump and laser wavelengths are taken into account. We consider that a single erbium ion placed into a fused silica matrix is described by a simplified five-level energy diagram [15]. Furthermore, we take into account that all waves traveling along the active single-mode step-index fiber (i.e. the pump, the laser and the amplified spontaneous emission (ASE) waves) are distributed by the Gaussian law with correspondent wave radii different for each wave. The z -dependent laser and ASE gains, pump absorption and ESA loss are calculated by integration of distributions of the correspondent waves' intensities over the homogeneously doped fiber core area [15,16], thus the radial distributions of populations of erbium ions being in different energy levels are taken into consideration. The model ignores polarization effects, interactions between neighboring erbium ions [17–19], and a possible difference of an erbium distribution from a rectangular form that coincides with the step-index fiber core. The model validity is confirmed by experiments on EDFL efficiency. The proposed model can be applied also for modeling EDFL in a ring configuration.

We also compare the proposed EDFL model with a simplified one, in which the radial distribution of erbium ions being in different energy levels is ignored (the plane distribution of populations, the PDP model). In this model the laser gain and the pump absorption are calculated as ones found on the fiber core axis multiplied by correspondent overlap factor (note that this simplification is usually used in FL models). We show that our model accounting for the radial distributions of populations of erbium ions (the RDP model) describes

* Corresponding author. Tel.: +52 477 4414200; fax: +52 477 4414209.
E-mail address: yuri@cio.mx (Y.O. Barmenkov).

FL much better than the simplified PDP model: in the RDP model the photon balance is satisfied automatically while a number of the actively absorbed pump photons differ from a number of all generated photons by approximately two times in the PDP model.

The paper is organized as follows: In Section 2 we refer to the set of the steady-state balance equations for the erbium-ion energy scheme used in modeling, along with definition of the relevant parameters. The laser equations are presented in Section 3. In Section 4, we consider some numerical examples of the distributed laser model and comparison with simplified ones. Some experimental results supporting the model are presented in Section 5. Finally, conclusions are given in Section 6.

2. Rate equations

We assume that the erbium ions in a silica fiber are described by a simplified five-level energy scheme presented in Fig. 1, each level is marked by the labels commonly used for energy manifolds of erbium ion and by the order number from the ion ground state. For our study we chose the fiber with low erbium concentration to ensure a negligible contribution from Auger up-conversion, the effect observed in heavy doped EDFs owing to the presence of erbium pairs [17–19]. The model accounts for all radiative and nonradiative transitions shown in this figure: the transitions $^4I_{15/2} \rightarrow ^4I_{11/2}$ and $^4I_{15/2} \rightarrow ^4I_{13/2}$ correspond to ground state absorption (GSA) at the pump ($\lambda_p = 976$ nm) and laser ($\lambda_s = 1550$ nm) wavelengths, respectively. The transitions $^4I_{11/2} \rightarrow ^4I_{15/2}$ and $^4I_{13/2} \rightarrow ^4I_{15/2}$ correspond to spontaneous emission (SE) at these wavelengths. ESA is described by the transitions $^4I_{11/2} \rightarrow ^4F_{7/2}$ at the pump wavelength and $^4I_{13/2} \rightarrow ^4I_{15/2}$ at the laser wavelength, these transitions are observed when levels “2” and “3” are not zero-populated. Close-lying levels $^4F_{7/2}$, $^2H_{11/2}$, and $^4S_{3/2}$ are regarded as the effective level “5”.

We consider that SE is originated from the ion relaxation corresponding to the $^4I_{13/2} \rightarrow ^4I_{15/2}$ transition. A part of SE power is captured by an active fiber core and is then amplified along the fiber. To simplify the model we suppose that SE has wavelength falling into the main SE absorption/emission peak ($\lambda_{se} = 1531$ nm), it is absorbed/amplified with the absorption/the gain coefficients measured at this wavelength. Otherwise one needs to decompose the absorption and gain spectra to a number of spectral components with corresponding amplitudes and spectral widths [20] and then to account each component separately in the laser equations. This simplification does not affect the laser model because the overall ASE power is much less than the laser power when pump level is substantially higher than the laser threshold, and the active fiber length is not too long.

Making these assumptions, the set of steady-state rate equations for continuous-wave lasers are given by Eqs. (1a)–(1e) [15].

$$\frac{\sigma_{12}^s I_s}{h\nu_s} N_1 + \frac{\sigma_{12}^{se} I_{se}}{h\nu_{se}} N_1 - \frac{\sigma_{21}^s I_s}{h\nu_s} N_2 - \frac{\sigma_{21}^{se} I_{se}}{h\nu_{se}} N_2 - \frac{\sigma_{24}^s I_s}{h\nu_s} N_2 - \frac{\sigma_{24}^{se} I_{se}}{h\nu_{se}} N_2 - \frac{N_2}{\tau_{21}} + \frac{N_3}{\tau_{32}} = 0 \quad (1a)$$

$$\frac{\sigma_{13} I_p}{h\nu_p} N_1 - \frac{\sigma_{31} I_p}{h\nu_p} N_3 - \frac{N_3}{\tau_{32}} - \frac{\sigma_{35} I_p}{h\nu_p} N_3 + \frac{N_4}{\tau_{43}} = 0 \quad (1b)$$

$$\frac{\sigma_{24}^s I_s}{h\nu_s} N_2 + \frac{\sigma_{24}^{se} I_{se}}{h\nu_{se}} N_2 - \frac{N_4}{\tau_{43}} + \frac{N_5}{\tau_{54}} = 0 \quad (1c)$$

$$\frac{\sigma_{35} I_p}{h\nu_p} N_3 - \frac{N_5}{\tau_{54}} = 0 \quad (1d)$$

$$N_1 + N_2 + N_3 + N_4 + N_5 = N_0 \quad (1e)$$

where h is the Plank constant, ν_p , ν_s and ν_{se} are the frequencies of the pump, signal (laser) and SE waves, σ_{ij} are the cross-sections for the

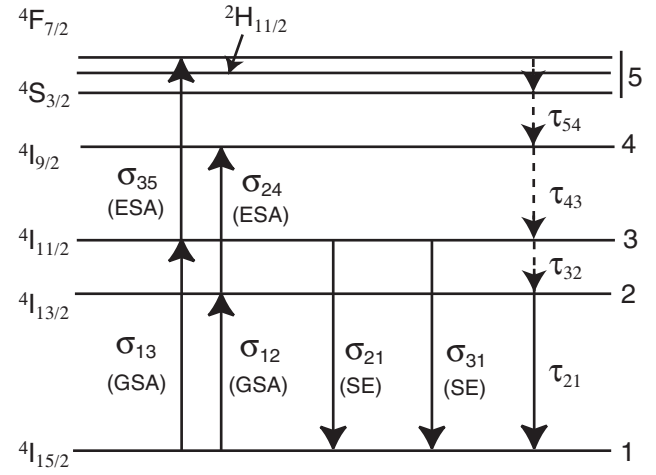


Fig. 1. Er^{3+} simplified energy-level diagram used in modeling. Photon-assisted transitions are shown by solid lines and thermal relaxation is marked by dash lines. σ_{ij} and τ_{ij} are, respectively, cross-sections and decay times for the transitions between the levels i and j .

transitions $i \rightarrow j$ (superscripts s and se indicate that the parameter refers to the signal or to the SE wavelength), τ_{ij} are the decay times between the levels i and j , I_p , I_s and I_{se} are the pump, signal and ASE waves' intensities, N_i are the populations of the correspondent Er^{3+} levels, N_0 is the Er^{3+} ions' concentration in the EDF core. (We considered that Er^{3+} ions are distributed homogenously over the fiber core and that the ions' concentration outside the core is zero).

To solve Eqs. (1a)–(1e), we introduce the notations for the normalized populations of the Er^{3+} levels: $n_i = N_i/N_0$. The solution can be obtained as follow:

$$n_1 = \begin{vmatrix} c_1 & a_{12} \\ c_2 & a_{22} \end{vmatrix} \bigg/ \begin{vmatrix} a_{11} & a_{12} \\ a_{21} & a_{22} \end{vmatrix}, \quad (2a)$$

$$n_2 = \begin{vmatrix} a_{11} & c_1 \\ a_{21} & c_2 \end{vmatrix} \bigg/ \begin{vmatrix} a_{11} & a_{12} \\ a_{21} & a_{22} \end{vmatrix}, \quad (2b)$$

$$n_3 = \frac{1 - n_1 - n_2}{1 + \varepsilon_p \gamma_2 s_p}, \quad (2c)$$

$$n_5 = \varepsilon_p \gamma_2 s_p n_3, \quad (2d)$$

where the matrices' coefficients are

$$a_{11} = (1 + \varepsilon_p \gamma_2 s_p)(s_s + s_{se}) - \gamma_1, \quad (3a)$$

$$a_{12} = -[1 + \gamma_1 + \varepsilon_p \gamma_2 s_p + [(\xi_s + \varepsilon_s)s_s + (\xi_{se} + \varepsilon_{se})s_{se}](1 + \varepsilon_p \gamma_2 s_p)], \quad (3b)$$

$$a_{21} = \gamma_1 + (1 + \xi_p)s_p + \varepsilon_p \gamma_2 s_p^2, \quad (3c)$$

$$a_{22} = (\varepsilon_s s_s + \varepsilon_{se} s_{se})(1 + \varepsilon_p \gamma_2 s_p) + (\gamma_1 + \xi_p s_p), \quad (3d)$$

$$c_1 = -\gamma_1, \quad (3e)$$

$$c_2 = \gamma_1 + \xi_p s_p, \quad (3f)$$

in that we use the next notations: $\varepsilon_p = \sigma_{35}/\sigma_{13}$, $\varepsilon_s = \sigma_{24}^s/\sigma_{12}^s$ and $\varepsilon_{se} = \sigma_{24}^{se}/\sigma_{12}^{se}$ are the pump, signal, and SE ESA parameters, $\gamma_1 = \tau_{21}/\tau_{32}$ and $\gamma_2 = \tau_{53}/\tau_{21}$ are the dimension-less temporal parameters, $\xi_p = \sigma_{31}/\sigma_{13}$ and $\xi_s = \sigma_{21}/\sigma_{12}$ are the coefficients characterizing the SE to GSA cross-sections' ratios at λ_p , λ_s and λ_{se} (λ_p , λ_s and λ_{se} are the

Download English Version:

<https://daneshyari.com/en/article/1537055>

Download Persian Version:

<https://daneshyari.com/article/1537055>

[Daneshyari.com](https://daneshyari.com)